

# CrystEngComm

Accepted Manuscript



This is an *Accepted Manuscript*, which has been through the Royal Society of Chemistry peer review process and has been accepted for publication.

*Accepted Manuscripts* are published online shortly after acceptance, before technical editing, formatting and proof reading. Using this free service, authors can make their results available to the community, in citable form, before we publish the edited article. We will replace this *Accepted Manuscript* with the edited and formatted *Advance Article* as soon as it is available.

You can find more information about *Accepted Manuscripts* in the [Information for Authors](#).

Please note that technical editing may introduce minor changes to the text and/or graphics, which may alter content. The journal's standard [Terms & Conditions](#) and the [Ethical guidelines](#) still apply. In no event shall the Royal Society of Chemistry be held responsible for any errors or omissions in this *Accepted Manuscript* or any consequences arising from the use of any information it contains.

## ARTICLE

# Template-free and green sonochemical synthesis of hierarchically structured CuS hollow microspheres displaying excellent Fenton-like catalytic activities

Cite this: DOI: 10.1039/x0xx00000x

Received 00th January 2012,  
Accepted 00th January 2012

DOI: 10.1039/x0xx00000x

www.rsc.org/

Chonghai Deng,<sup>\*ab</sup> Xinqing Ge,<sup>c</sup> Hanmei Hu,<sup>\*c</sup> Li Yao,<sup>a</sup> Chengliang Han,<sup>a</sup> and Difang Zhao<sup>a</sup>

Hierarchically structured hollow microspheres composed of copper sulfide (CuS) nanoplatelets have been successfully fabricated via a one-pot and green sonochemical process for the first time, using copper acetate and thiourea aqueous solution as precursor without surfactant and template. Large-scaled hollow architectures with out-diameters in the range of 1~1.2  $\mu\text{m}$  are assembled by pure hexagonal single crystalline CuS nanoplatelets, being of about 20 nm in thickness with stacking faults in crystal lattice. The UV-Vis diffuse reflectance spectra (DRS) analysis suggests that the band gap energy of as-obtained CuS sample was estimated to be 1.27 eV, showing a significant red-shift compared with the value of bulk. Hollow CuS structures possess the high surface area and the double pore size distributions measured from the  $\text{N}_2$  adsorption isotherms. Moreover, the possible growth mechanism for CuS hollow spheres is proposed on the basis of the temporal evolution controlled experiments. More importantly, this hierarchically structured CuS catalysts show highly efficient Fenton-like catalytic activities in degrading highly concentrated dye-containing solution ( $50\text{mg}\cdot\text{mL}^{-1}$ ) with the help of hydrogen peroxide ( $\text{H}_2\text{O}_2$ ), suggesting a promising application in wastewater purification.

## 1. Introduction

Copper sulfide (CuS), as an important transition-metal sulfide, has been the focus of considerable attention because of not only its excellent electrical, optical, physical and chemical properties but also its potential applications in many fields, such as superconductor at low temperature, solar energy converter, cathode material, catalyst, optical filter, gas sensing material and nonlinear optical material.<sup>1-3</sup> As is known, the morphology as well as the chemical composition of nano/microstructures has great effect on their properties and promising applications. The uniform sizes and morphologies of nano/microstructures have a serious of physicochemical properties being different from the bulk. In particular, the hierarchically structured hollow spheres are stimulated extensive interest due to their unusual structural features, including low density, high surface area, good permeation and outstanding optical/electrical behaviors,<sup>4,5</sup> which make them promising for their potential applications in drug-delivery systems,<sup>6</sup> lithium-ion batteries,<sup>7</sup> catalysts,<sup>8,9</sup> gas sensors,<sup>10</sup> and absorbents.<sup>11</sup> The conventional approaches to preparation of the hollow structures have involved the use of various removable or sacrificial templates and/or surfactants, including hard ones (e.g., silica spheres, carbon spheres, and metal nanoparticles),<sup>4,5</sup> and soft ones (e.g., micelles, emulsion droplets, liquid drops, and even bacteria).<sup>12-14</sup> As for CuS semiconductor, a diverse portfolio of hollow structures were prepared by template methods and typically physicochemical routes.<sup>15-25</sup> But the above-mentioned approaches to fabrication

of hollow CuS structures might inevitably increase the reaction complexity, suffer tedious synthetic procedures, cause impurity in the products. There is no doubt that the *in situ* "gas-bubbles" template strategy enjoys the advantage of avoiding the template removal step in the hollow materials preparation, which sounds more fascinating and prospective. Up to date, there are countable reports on the preparation of hollow CuS spheres employing "gas-bubbles" as soft templates. For example, Hu *et al.*<sup>26</sup> and Chen *et al.*<sup>27</sup> have obtained CuS hollow spheres using  $\text{CO}_2$  bubbles as template under hydrothermal conditions. Xue and Liu have synthesized hollow CuS spheres by self-assembly coupled with  $\text{H}_2\text{S}$  bubbles templating *via* solvothermal route.<sup>28</sup> Hu and his colleagues have developed a general bubble-templating method to fabrication of transition metal sulfides hollow spheres, such as CuS, CdS, ZnS and  $\text{Bi}_2\text{S}_3$ .<sup>9</sup> However, those hydro/solvothermal methodologies have ineluctable high-cost and time-consuming, and is disadvantageous from the viewpoint of green chemistry. Thus it is still a challenge to explore a novel green chemistry route for synthesis of hollow structures with their promising applications. To the best of our knowledge, there is no report on the fabrication of CuS hollow structures by the template-free and ultrasound-assisted aqueous chemical process.

In recent years, considerable attention has been paid to the environmental pollutants including industrial wastewater treatment. Industrial wastewater is predicted to become a major threat to human beings and becomes one of the most critical environmental problems already. Dye-containing wastewater

contains a large amount of recalcitrant toxic substances, such as azo and benzol groups, which is contributed to an increasing risk in the incidence of bladder cancer among humans. In order to degrade those toxic substances in dye wastewater, the method of  $\text{H}_2\text{O}_2$  catalytic oxidation, with transition metal chalcogenides as catalysts releasing highly reactive hydroxyl radicals, has been proven to be effective in treating dye-containing wastewater.<sup>29-33</sup> In such a process,  $\text{H}_2\text{O}_2$  is decomposed and highly reactive hydroxyl radicals ( $\bullet\text{OH}$ ) are generated. These non-selective species are among the most oxidizing known compounds and are able to degrade a wide range of organic pollutants to convert organic macromolecules into small pollution-free molecules,  $\text{CO}_2$ , and  $\text{H}_2\text{O}$ . As is popularly believed, the hierarchically structured catalysts can avoid aggregation and maintain the high specific surface areas which play an important role in their accessibility of adsorbates to reactive sites, displaying structural enhanced adsorption properties and high decolorization degree for dye pollutants.<sup>34,35</sup> Generally, hierarchical copper-based chalcogenide catalysts have been often studied to decolorize and/or photodegrade organic dyes solution, in which methylene blue (MB) and Rhodamine B (RhB) are employed as probe molecules.<sup>36-41</sup> For example, Li and his colleagues have reported the hierarchical CuS architectures with the enhanced peroxidase-like catalytic activities for the dyes degradation with the assist of  $\text{H}_2\text{O}_2$ .<sup>30,31</sup>

In our work, for the first time, a template-free and green sonochemical approach is presented to fabricate the hierarchical CuS hollow spheres. The hierarchical structures with hollow interior stacked by single-crystal covellite CuS nanoplatelets are successfully synthesized by sonicating an aqueous solution of copper acetate and thiourea in the closed system in the absence of any surfactant and template. In addition, the possible growth mechanism for hierarchical CuS hollow structures is proposed, as is considered as an *in situ* "bubble-templating" oriented aggregation and growth under sonolysis based on the temporal evolution controlled experiments. More importantly, for developing the practical applications in the environmental remediation, the as-obtained hierarchical CuS hollow sphere as a catalyst is employed in catalyzed oxidative decomposition of  $\text{H}_2\text{O}_2$  at the lower quality concentration (0.5 mL) for high-concentration (50  $\text{mg}\cdot\text{L}^{-1}$ ) methylene blue (MB) or rhodamine B (RhB) dyes aqueous solution, exhibiting highly efficient heterogeneous catalysts for dyes decolorization.

## 2. Experimental

### 2.1. Sample preparation

The sonochemical reactions were implemented in a locally supplied ultrasonicator (KQ-50, 40 kHz, 50 W). Copper acetate monohydrate ( $\text{Cu}(\text{CH}_3\text{COO})_2\cdot\text{H}_2\text{O}$ ), thiourea ( $\text{H}_2\text{NCSNH}_2$ , TU) and commercial CuS were all analytical-grade purity and purchased from Sinopharm chemical reagent company. All the chemicals were used as received without further treatment. Distilled water was used to prepare the solution. In a typical experimental procedure for CuS hollow structures, 1 mmol  $\text{Cu}(\text{CH}_3\text{COO})_2\cdot\text{H}_2\text{O}$  (0.1994 g) and 4 mmol TU (0.2999 g) were dissolved in 60 mL distilled water under continuous stirring. Subsequently, the precursor solution containing autoclavable bottle (100 mL) was sealed with the attached screw cap to form a closed system, and then transferred into a sonication bath with the temperature of water bath at 80 °C without stirring. After the ultrasound radiation was performed for 60 min, the reaction mixture solution was cooled naturally for overnight. The resulting black precipitate was filtered with a microporous membrane with pores of 0.45  $\mu\text{m}$  in diameter, washed by distilled water and anhydrous

ethanol for several times to remove residuals. The grey-black products were finally obtained after dried in a vacuum at 60 °C for 6 h.

### 2.2. Characterization

The phase structure and phase purity of as-prepared sample was measured on a Theta/Theta Rotating anode X-ray diffractometer (XRD, Rigaku TTR-III, 18KW,  $\lambda=1.5418$  Å) using standard Cu K $\alpha$  radiation. The surface morphologies were determined on a field emission scanning electron microscope (FESEM, JEOL-6700F), and a high-resolution transmission electron microscope (TEM, JEOL JEM-2010). Elemental analysis was conducted using an energy-dispersive X-ray (EDX) detector attached to FESEM. UV-Vis diffuse reflectance spectra (DRS) were recorded on a UV-Vis spectrophotometer (Solidspec-3700 DUV) at room temperature. Nitrogen ( $\text{N}_2$ ) adsorption/desorption isotherms were measured by using an Rristar II 3020M Analyzer.

### 2.3. Catalytic activity evaluation

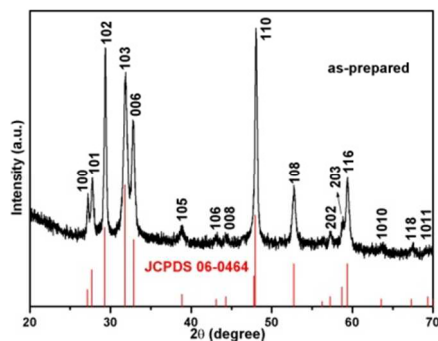
The evaluation of the catalytic activity of as-prepared products for the catalytic decolorization of dye aqueous solution was performed at room temperature. The degradation experiments were carried out in a slurry reactor containing 20 mg of catalyst, 20 mL of a 50  $\text{mg}\cdot\text{L}^{-1}$  MB (or RhB) aqueous solution. Prior to introduction of  $\text{H}_2\text{O}_2$ , the suspension was kept in the dark under stirring for 30 min to ensure the establishment of an adsorption-desorption equilibrium. The reaction proceeded at ambient temperature with slowly stirring and initiated by adding 0.5 mL of 30% hydrogen peroxide. At given time intervals, the suspension was sampled 1 mL and diluted to 5 mL by adding 4 mL distilled water, and then was centrifuged immediately for the following analysis. The concentration of dye left in the centrifuged aqueous solution was determined by a UV-visible spectrophotometer (PerkinElmer Lambda 950) in the wavelength range of 220-800 nm, from which the degradation efficiency was evaluated. For comparison, the catalytic performance of commercial CuS powder was also tested at the same experimental conditions, in order to highlight the highly efficient activity of the hierarchical CuS hollow spheres.

## 3. Results and discussion

### 3.1. Morphologies and chemical composition analysis

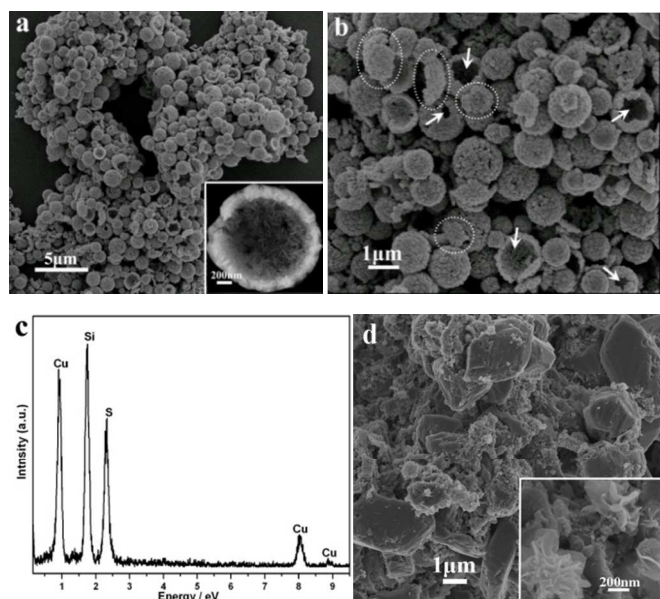
The X-ray diffraction test was carried out to understand the identity and phase of as-resulting products. As is depicted in Fig. 1, the peaks in the diagram is in good agreement with the standard data from JCPDS card No. 06-0464, and is assigned to the pure hexagonal phase CuS with the  $\text{P6}_3/\text{m}$  space group and a primitive hexagonal unit cell with  $a = b = 3.792$  and  $c = 16.344$  Å. The strong and sharp diffraction peaks indicate the good crystallinity. No other obvious peaks of impurities are observed in the sample, indicating the high purity of CuS prepared by a template-free and one-pot green sonochemical process.





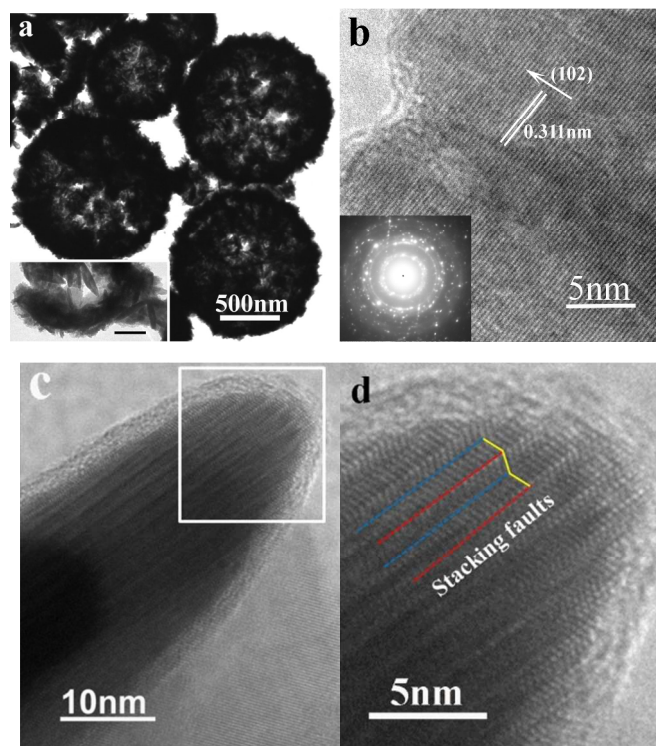
**Fig. 1** Typical XRD pattern of as-prepared CuS products.

Fig. 2 displays the morphologies and the energy dispersive X-ray (EDX) analysis of as-obtained sample. From the low-magnification FESEM image (Fig. 2a), it can be found that the large-scaled monodispersed CuS architectures are almost the three-dimensional (3D) microspherical structures with the out-diameters in the range of 1~1.2  $\mu\text{m}$ . As shown in Fig. 2b, the high-magnification FESEM image clearly displays that there are dominant hollow spheres, several cave-in and half hollow spheres (indicated by the white arrows) as well as some pieces of broken shells (indicated by the white dot circles) in the products. From a representative hollow half-sphere (inset of Fig. 2a), the interior of hollow morphology is plainly visible and the inner surface shows a protrusive structure. Upon closer examination, the walls of spherical-shell with a thickness of about 200 nm are self-assembled by cross-bedded nanoplatelets with around 20 nm in thickness. Additionally, the results of EDX analysis (Fig. 2c) show that the peaks of Cu and S element are observed without any other peak (the Si peak is due to background from Si foil), and the atomic ratio of Cu:S is 30.30:30.65 - close to 1:1, which is in agreement with the stoichiometric ratio of CuS. Thus the hierarchical hollow spherical structures are further considered as pure CuS, being consistence of XRD results. Moreover, the FESEM image of commercial CuS is given in Fig.2d, from which one can see a few irregular microparticles as well as a plenty of nanoflowers aggregated by nanoplatelets (inset of Fig.2d).



**Fig. 2** (a and b) FESEM images, and (c) EDX analysis of as-prepared CuS products, (d) FESEM image of commercial CuS.

The further detailed structural characterizations of hollow CuS were investigated by TEM and HRTEM. The strong contrast between the dark edge and pale center is the obvious evidence for their hollow nature in Fig. 3a. From the high-magnification TEM image of a small piece of broken spherical-shell (inset of Fig. 3a), it is clear that the shell of the hollow microsphere is composed of nanoplatelets, being in agreement with FESEM results. The HRTEM images conducted on the scattered nanoplatelet are given in Fig.3b and c. From the top-view HRTEM image (Fig. 3b), the regular spacing of the clear lattice planes is calculated to be 0.311 nm, which is in good agreement with the interlayer spacings of (102) crystallographic plane of hexagonal CuS, being consistent with the orientation of the nanoplatelet reported by Li *et al.*<sup>37</sup> The corresponding SAED pattern (inset of Fig. 3b) is characterized as discrete spots and electron diffraction rings, which indicates the both single-crystalline and polycrystalline feature of CuS.<sup>42</sup> The weak satellite diffraction spots are resulted from the presence of crystals defects with specific crystalline orientations.<sup>43</sup> The side-view HRTEM image (Fig. 3c) further confirms that the thickness of nanoplatelet is about 20 nm, and the stacking faults in the crystals are clearly observed from the ravines and gullies on the crystal side-surface. A closer observation from the zoomed HRTEM of Fig. 3d (taken from the area marked with square in Fig. 3c) demonstrates that obvious planar defect structures as typical polysynthetic twinning planes are formed.<sup>23,43</sup> Based on the above structural characterization, it can draw a conclusion that the hierarchically structured hollow microspheres are self-assembled by single crystalline CuS nanoplatelets containing stacking faults of crystals defects.



**Fig. 3** (a, the scale bar in the inset: 200nm) TEM image and (b-d) HRTEM images of as-prepared CuS hollow microspheres.

The Uv-Vis diffuse reflectance spectrum (DRS) of as-prepared CuS hollow spheres was examined at room temperature. As shown in Fig. 4, the Uv-Vis absorption spectrum reveals that a rather weak

absorption peak is centered at about 670 nm in the visible region, as well as a broader tailer lies in the near IR (NIR) ranging from 800 to 1200 nm. It can be deduced that CuS hollow microspheres lead to the broadening of optical absorption in the visible and NIR region, which shows great potential applications in the fields of photocatalytic and solar cells. Furthermore, the optical absorption near the band gap  $E_g$  has been calculated using Tauc's formula:  $(\alpha h\nu)^n = A(h\nu - E_g)^{4n}$ , where  $A$  is a constant, and the exponent  $n$  is equal to 2 for the allowed direct transitions. The  $(\alpha h\nu)^2 \sim h\nu$  curve for CuS hollow microspheres is given in the insert of Fig. 4, exhibiting one plot of linear relationship between 1.55 and 1.80 eV. The band gap  $E_g$  is estimated to be 1.27 eV from the onset of the absorption edge. There is a significant red-shift in the as-obtained CuS hollow microspheres compared with the value of bulk CuS for which it is 1.85 eV.<sup>38</sup> This red-shift phenomenon is attributed to the enhanced internal stress originating from the hollow structures which may be induced by the structural defects, and the enhanced internal stress results in the overlap of the electron wave function generated in the process of aggregation and assembly.<sup>23,45</sup>

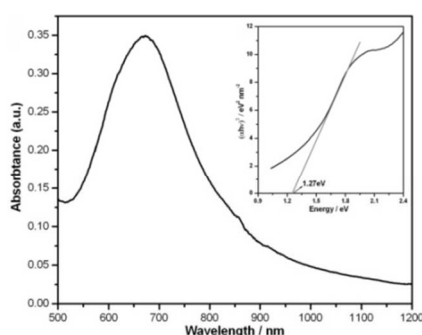


**Fig. 4.** UV-vis absorption spectrum and  $(\alpha h\nu)^2 \sim h\nu$  curve (inset) of as-prepared hierarchical CuS hollow structures.

The Brunnauer-Emmett-Teller (BET) gas sorptometry measurement was conducted to illustrate the porous structure of as-obtained hierarchical CuS hollow microspheres. The nitrogen adsorption/desorption isotherm and corresponding BET pore size distribution are illustrated in Fig. 5. According to Brunauer-Deming-Deming-Teller (BDDT) classification, the isotherm is identified as typical type IV, which indicates a hysteresis loop characteristic of mesoporesity (2-50 nm).<sup>46</sup> The inset of Fig. 5 is the corresponding Barrett-Joyner-Halenda (BJH) pore size distribution curve. The double pore structures were observed and the pore sizes were calculated to be 10.4 and 18.8 nm in diameter, respectively. In addition, the BET specific surface area was measured to be 25.4 m<sup>2</sup>/g. The unique double pore structures and the considerable high surface area can make it a promising candidate as a catalyst for the degradation dye pollutions in wastewater.

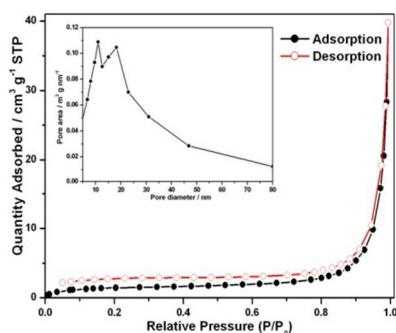
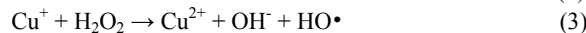


**Fig. 5** N<sub>2</sub> adsorption-desorption isotherm and pore size distribution curve (inset) of hierarchical CuS hollow spheres.

### 3.2. Decolorization of high-concentration dyes solution

Owing to the special porous and hierarchical structure with hollow interior, the CuS hollow spheres were used as the catalysts for adsorption/degradation of organic dyes, such as MB and RhB molecules, and the related experiments were carried out with the addition of H<sub>2</sub>O<sub>2</sub>. In the catalytic process, H<sub>2</sub>O<sub>2</sub> reacted with the catalyst to yield highly reactive hydroxyl radicals ( $\cdot\text{OH}$ ) that could oxidize organic substrate (RH) into smaller molecules (CO<sub>2</sub>, H<sub>2</sub>O, etc.). As is proven, H<sub>2</sub>O<sub>2</sub> alone was not capable of degrading dye solutions without the assistance of the catalyst, and at the same time, only CuS catalyst can contribute none to the catalytic efficiency.<sup>30,31</sup> A brief description of the reaction mechanism could be described below according to the recently reports of Li's contributions:<sup>30,47</sup>



HO $\cdot$  radicals can attack an organic substrate RH:



In our reaction system, the amount of CuS catalyst was 20 mg at MB and RhB dyes concentration of 50 mg·L<sup>-1</sup> (20 mL) and H<sub>2</sub>O<sub>2</sub> dosage of 0.5 mL. The control experiments further demonstrate that the presence of both catalyst and H<sub>2</sub>O<sub>2</sub> is necessary for efficient degradation (see lines v and vi in Fig.6c). Significantly, the catalytic behaviors of as-prepared CuS hollow microspheres show the high efficient catalysis of H<sub>2</sub>O<sub>2</sub> to release  $\cdot\text{OH}$  and degrade high-concentration dyes solution in a short time. The evolutions in UV-vis spectra during the decolorization of MB and RhB over as-obtained hollow CuS are illustrated in Fig. 6a and b, respectively. From Fig. 6a, the decoloring rate of aqueous MB reached 45.3% within the initial 1 min; and after 5 min, the decoloring degree was up to 82.8%; the total decoloring degree achieved 95.6% within 30 min. From Fig. 6b, the decoloring degree of RhB solution reached 68.3% after 5 min; and the total decoloring rate was up to 90.7% after 40 min and then was maintained at a relatively stable level. In previous reports, the dyes concentrations typically are 5 or 10 mg·L<sup>-1</sup> to evaluate the catalytic performances of the catalysts.<sup>30,36</sup> In contrast to earlier studies, the time consumed in using as-prepared CuS hollow microspheres to decolorize 10 mg/L MB in the present study was lower than 5 min at the same manner. Moreover, to the best of our knowledge, no reports have yet discussed the hollow hierarchical CuS microspheres as a Fenton-like catalyst for degrading such a high-concentration of dyes solution. For further highlighting the excellent catalytic performance over as-prepared hollow CuS architectures, the commercial CuS powder was selected to test its catalytic activities at the same experimental conditions. The changes of UV-vis spectra during the removal of MB and RhB over commercial CuS catalysts are shown in Fig. 6c and d, respectively. And the time profiles of corresponding decolorization rates are drawn by lines iii and iv in Fig.6e. Obviously, the total decoloring degrees over commercial CuS powders were only 46.4% and nearly 40% for MB and RhB within the equal time, respectively. Thus it can be seen that the hollow CuS architectures possess the superior removal capacities for the simulated pollutants in the wastewater far more efficiently than that of the commercial CuS, due to the unique hierarchical and hollow features.

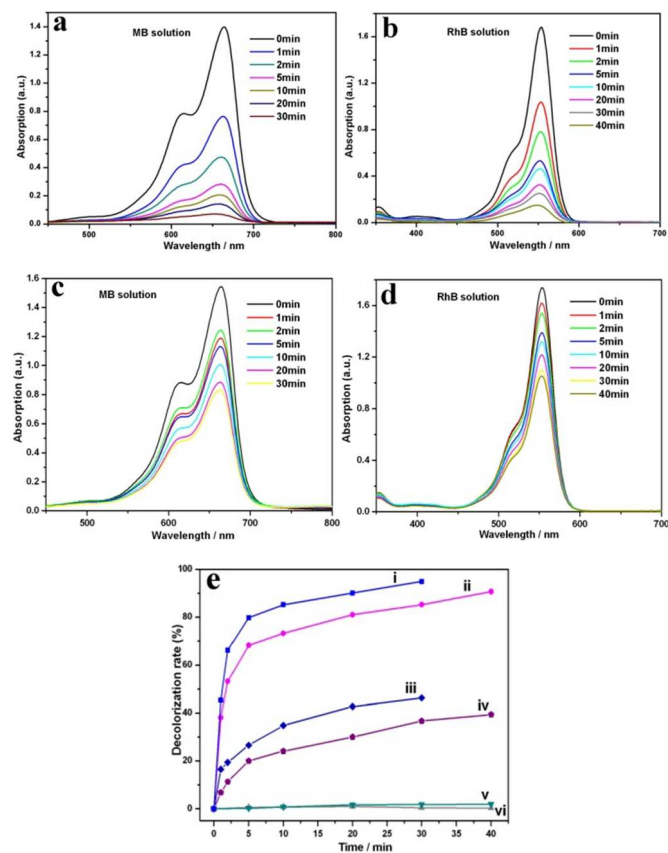


**Fig.6** The changes of UV-vis spectra during the removal of different dyes over as-prepared hollow CuS catalysts (a: MB; b: RhB) and commercial CuS powders (c: MB; d: RhB), and (e) the time profiles of the decoloration of dyes under different conditions (i: for CuS hollow spheres with  $\text{H}_2\text{O}_2$  in degrading MB; ii: for CuS hollow spheres with  $\text{H}_2\text{O}_2$  in degrading RhB; iii: for only  $\text{H}_2\text{O}_2$  without catalyst in degrading MB; iv: for only CuS hollow spherical catalyst without  $\text{H}_2\text{O}_2$  in degrading MB; v: for commercial CuS powders with  $\text{H}_2\text{O}_2$  in degrading MB; vi: for commercial CuS powders with  $\text{H}_2\text{O}_2$  in degrading RhB.).

Considering that the stability of catalysts is important to their applications, the recycled catalytic experiments were carried out 5 times under the same conditions, and Fig. 7 illustrated the profiles of cyclic tests of the catalytic degradation. As shown in the upper of Fig. 7, the degradation rates largely stand  $\sim 90\%$  for MB after 30 min. The first degradation degree reached 95.6%, and after repeating the procedure five more times, the decoloring rate remained at 89.7%. Whereas for RhB solution (lower of Fig. 7), the degradation rates slightly decreased but maintained the high level after 40 min. The degradation rate was still nearly 80% after five recycles. Thereby, those demonstrate that the as-prepared CuS hollow architectures is believed to be potentially effective in dyes decolorization, which enable the attractive candidate as a practical catalyst for water purification.

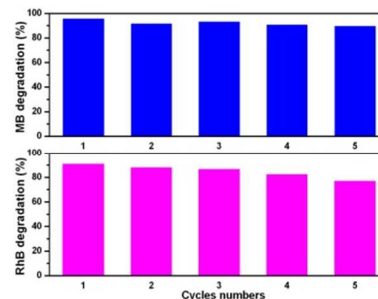
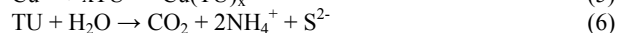
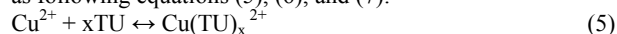


**Fig.7** The profiles of five cyclic catalytic tests in degradation of MB (upper) and RhB (lower) over as-obtained hollow CuS catalysts with  $\text{H}_2\text{O}_2$ .

### 3.3. Plausible growth mechanism of hierarchical CuS hollow microspheres

TU is a commonly used sulfide source for syntheses of transition metal chalcogenides in aqueous process. TU molecule has lone pair of electrons on nitrogen and sulfur atoms, which has the great coordinating ability with metals in  $\text{M}^{n+}$  to form  $\text{M}(\text{TU})_x^{n+}$  complexes.<sup>27</sup> Therefore,  $[\text{Cu}(\text{TU})_x]^{2+}$  complexes can also yield promptly as TU is added into the blue aqueous solution containing  $\text{Cu}^{2+}$  ions under stirring.<sup>27</sup> While the solution of TU is heated at the temperature of  $80^\circ\text{C}$ , TU can decompose to produce carbon dioxide ( $\text{CO}_2$ ) and active  $\text{S}^{2-}$  ions into the aqueous solution,<sup>16,27</sup> which can drive  $[\text{Cu}(\text{TU})_x]^{2+}$  complexes to gradually release  $\text{Cu}^{2+}$  ions. Thus newly-dissociated  $\text{Cu}^{2+}$  reacts with active  $\text{S}^{2-}$  immediately to generate CdS nuclei. The main chemical reactions can be expressed as following equations (5), (6), and (7).<sup>27,48</sup>



The sonochemistry is based on acoustic phenomenon resulting from the continuous formation, growth and implosive collapse of bubbles in the aqueous solution, which can achieve extreme high temperature ( $>5000\text{ K}$ ) and high pressure ( $>20\text{ MPa}$ ) and very high cooling rates ( $10^{10}\text{ K}\cdot\text{s}^{-1}$ ) upon the collapse of bubbles. The radical species can generate from the water molecules which decompose in the inner gas phase of the collapsing bubbles.<sup>49</sup> So on the ultrasound conditions, TU molecule decomposition can be boosted to generate  $\text{CO}_2$  gas and  $\text{S}^{2-}$  anions, and simultaneously the crystal nucleation rate of CuS can be accelerated further. Thus plenty of nanoparticles of covellite CuS were obtained sonochemically from copper acetate and TU aqueous solution in the open system, which is reported by Kristl's group.<sup>50</sup> It is demonstrated clearly that the hollow structure of CuS cannot be fabricated under the ambient air by the sonolysis proceeding. That is, in the open condition, the  $\text{CO}_2$  bubbles decomposed from TU do not work as templates for the help of preparation of the hollow structures, which collapse and escape from the body solution contributed to the degassing effect of ultrasound wave. While in our pre-designed closed system, the hierarchical CuS hollow microspheres were successfully fabricated by sonolysis the same precursor solution, which is considered as an ingenious strategy. Because of in the closed condition, the newly-produced  $\text{CO}_2$  microbubbles can be detained in the reaction solution under the saturated steam pressure, in this regard, which is similar to the hydrothermal process at the low temperature.<sup>27</sup> Thus, lots of  $\text{CO}_2$  microbubbles just generated and detained in the aqueous solution can act as the aggregation centers, to help the primary CuS nuclei to format and aggregate on the gas-liquid interface of the solution between  $\text{CO}_2$  and water. And it is not impossible to fabricate the hollow microspheres employing  $\text{CO}_2$  microbubbles as "template" in the sonolysis process, just another example of the hierarchical CuO



hollow architectures reported by our previous study.<sup>42</sup>

Further, the growth and morphology evolution process of the hierarchical CuS hollow microspheres was also revealed by the temporal variation controlled experiments. Fig. 8 show the FESEM images of the CuS products obtained at different reaction stages. As the reaction time was 5 min, the poor harvests of the agglomerates assembled by tiny nanoparticles were collected (Fig. 8a). When the sonication time is 20 min, CuS nanograins were oriented aggregation and growth on the gas-liquid interface of the solution between CO<sub>2</sub> and water, tending to assemble into hollow spherical structures with the diameter of about 200–300 nm (Fig. 8b), of which the interior surface is nicely compact and perfect geometrical symmetry (the inset of Fig.8b). It is demonstrated that the CO<sub>2</sub> gas bubbles have been introduced as “template” to help the CuS nuclei oriented aggregation and growth. While the sonication time extended to 30 min, lots of hollow spheres were collapsed (Fig.8c), which suggests that the interior of CuS hollow structures formatted previously were subjected to gradually dissolution in order to supply configurational ions for recrystallization. With the extension of sonication time to 40 min, larger and integrated submicrospheres with the diameter of 500 nm were obtained during the secondary growth (Fig. 8d). While the sonication time reached 60 min, the hierarchical CuS hollow microspheres with the out-diameters in the range of 1~1.2 μm are formed finally through the sufficient secondary growth and Ostwald ripening process (Fig. 2a and b). The walls of hollow architectures are composed of nanoplatelets with intersection, which is determined by the intrinsic crystal characteristics of the hexagonal CuS, because the formation of nanoplatelets is more readily available under the appropriate conditions.<sup>30,31,36</sup> Based on the above analysis and results, the schematic diagram and plausible formation mechanism for hierarchical CuS hollow structures is illustrated in Fig. 9, as is considered as a sonohydrolysis - oriented aggregation - secondary growth and ripening process.

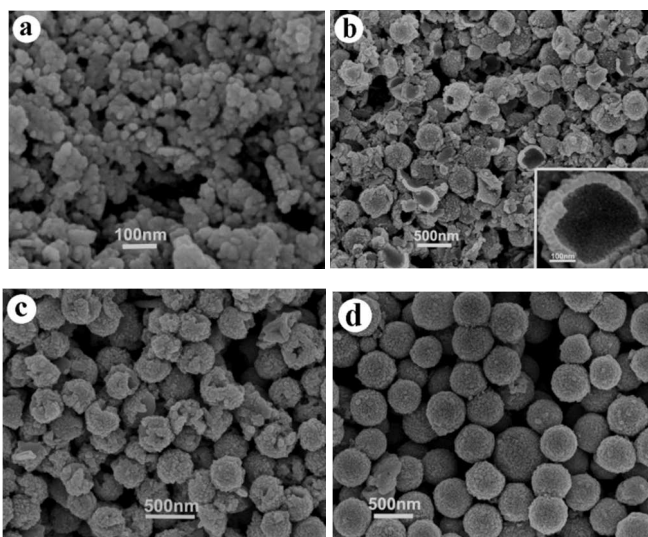


**Fig. 8.** FESEM images of CuS samples at different reaction times. (a) 5 min; (b) 20 min; (c) 30 min; (d) 40 min.

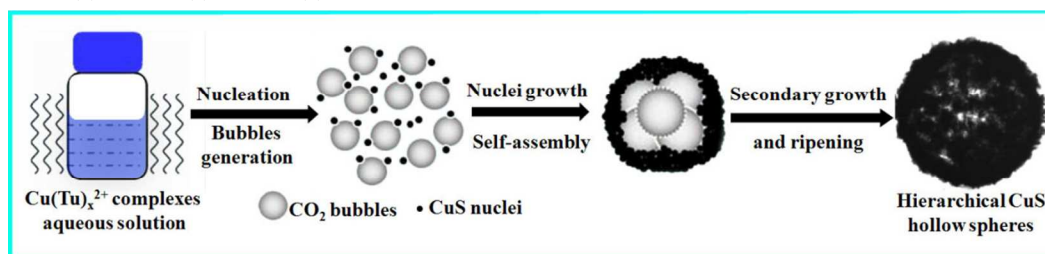


**Fig. 9.** Plausible schematic illustration of formation of the hierarchical CuS hollow spheres.

#### 4. Conclusions

A template-free and green sonochemical synthetic technology is demonstrated to construct hierarchically structured CuS hollow spheres in the absence of any template and additive. The as-prepared CuS products exhibit uniform geometrical shapes with hollow features, and their walls are self-assembled by single crystalline nanoplatelets with stacking faults in crystal lattice. The plausible formation mechanism for hollow CuS architectures is also presented. Significantly, the as-synthesized hierarchical CuS structures displayed excellent peroxidase-like activities to decolorize the highly concentrated dye-containing solution with the assist of H<sub>2</sub>O<sub>2</sub>, which can further develop their promising application in removal of organic pollutants for environmental remediation. Of course, it is also expected to be useful in many other applications, such as solar energy cells, optical and electronic materials, and so forth. Additionally, the present one-pot green sonochemistry technology would be readily applicable to the creation of other hierarchical and hollow inorganic functionalized nanomaterials toward their specific applications.

#### Acknowledgements

The first author Dr. Chonghai Deng is grateful to Prof. Yi Xie (University of Science & Technology of China) for her help, and this work was supported by the National Natural Science Foundation of China (11079004, 10979047 and 11135008), and the Fifth Science and Technology Foundation of Outstanding Youth of Anhui Province (1308085JGD06).

#### Notes and references

<sup>a</sup> Department of Chemical and Materials Engineering, Hefei University, Hefei, 230022, P. R. China. E-mail: chdeng@mail.ustc.edu.cn.

<sup>b</sup> Hefei National Laboratory for Physical Sciences at Microscale, University of Science and Technology of China, Hefei, 230026, P. R. China. E-mail: chdeng@mail.ustc.edu.cn.

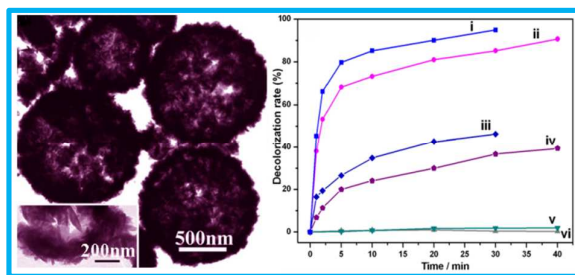
<sup>c</sup> School of Materials and Chemical Engineering, Anhui Jianzhu University, Hefei, 230026, P. R. China. E-mail: hmhu@ustc.edu.

- 1 M. Zhou, R. Zhang, M. Huang, W. Lu, S. L. Song, M. P. Melancon, M. Tian, D. liang and C. Li, *J. Am. Chem. Soc.*, 2010, **132**, 15351-15358.
- 2 J. Liu and D. F. Xue, *J. Mater. Chem.*, 2011, **21**, 223-228.
- 3 Y. Zhang, J. Tian, H. Li, L. Wang, X. Qin, A. M. Asiri, A. O. Al-Youbi and X. Sun, *Langmuir*, 2012, **28**, 12893-12900.
- 4 X. L. Xu and S. A. Asher, *J. Am. Chem. Soc.*, 2004, **126**, 7940-7945.
- 5 J. S. Zhou, H. H. Song, X. H. Chen, L. J. Zhi, S. B. Yang, J. P. Huo and W. T. Yang, *Chem. Mater.*, 2009, **21**, 2935-2940.

- 6 J. Liu, S. Z. Qiao, S. B. Hartono and G. Q. Lu, *Angew. Chem. Int. Edit.*, 2010, **49**, 4981-4985.
- 7 X. W. Lou, Y. Wang, C. L. Yuan, J. Y. Lee and L. A. Archer, *Adv. Mater.*, 2006, **18**, 2325-2329.
- 8 J. G. Yu and X. X. Yu, *Environ. Sci. Technol.*, 2008, **42**, 4902-4907.
- 9 M. Luo, Y. Liu, J. C. Hu, J. L. Li, J. Liu and R. M. Richards, *Appl. Catal. B Environ.*, 2012, **125**, 180-188.
- 10 W. S. Choi, H. Y. Koo, Z. Zhongbin, Y. Li and D. Y. Kim, *Adv. Funct. Mater.*, 2007, **17**, 1743-1749.
- 11 Y. Q. Wang, G. Z. Wang, H. Q. Wang, W. P. Cai, C. H. Liang and L. D. Zhang, *Nanotechnol.*, 2009, **20**, 155604-155609.
- 12 F. Caruso, R. A. Caruso and H. Mohwald, *Science*, 1998, **282**, 1111-1114.
- 13 Q. Liu, H. Liu, M. Han, J. Zhu, Y. Liang, Z. Xu and Y. Song, *Adv. Mater.*, 2005, **17**, 1995-1999.
- 14 D. Walsh, B. Lebeau and S. Mann, *Adv. Mater.*, 1999, **11**, 324-328.
- 15 S. M. Wan, F. Guo, L. Shi, Y. Y. Peng, X. Z. Liu, Y. G. Zhang and Y. T. Qian, *J. Mater. Chem.*, 2004, **14**, 2489-2491.
- 16 J. Z. Xu, S. Xu, J. Geng, G. X. Li and J. J. Zhu, *Ultrason. Sonochem.*, 2006, **13**, 451-454.
- 17 S. H. Jiao, K. Jiang, Y. H. Zhang, M. Xiao, L. F. Xu and D. S. Xu, *J. Phys. Chem. C*, 2008, **112**, 3358-3361.
- 18 X. L. Yu, Y. Wang, H. L. W. Chan and C. B. Cao, *Micropor. Mesopor. Mater.*, 2009, **118**, 423-426.
- 19 H. T. Zhu, J. X. Wang and D. X. Wu, *Inorg. Chem.*, 2009, **48**, 7099-7104.
- 20 L. Ge, X. Y. Jing, J. Wang, S. Jamil, Q. Liu, D. L. Song, J. Wang, Y. Xie, P. P. Yang and M. L. Zhang, *Cryst. Growth Des.*, 2010, **10**, 1688-1692.
- 21 D. H. Jiang, W. B. Hu, H. R. Wang, B. Shen and Y. D. Deng, *J. Colloid Interf. Sci.*, 2011, **357**, 317-321.
- 22 D. H. Jiang, W. B. Hu, H. R. Wang, B. Shen and Y. D. Deng, *Colloid Surf. A: Physicochem. Eng. Asp.*, 2011, **384**, 228-232.
- 23 S. D. Sun, X. P. Song, C. C. Kong, S. H. Liang, B. J. Ding and Z. M. Yang, *CrystEngComm*, 2011, **13**, 6200-6205.
- 24 S. S. Dhasade, S. Patil, B. B. Kale, S. H. Han, M. C. Rath and V. J. Fulari, *Mater. Lett.*, 2013, **93**, 316-318.
- 25 X. Y. Meng, G. H. Tian, Y. J. Chen, R. T. Zhai, J. Zhou, Y. H. Shi, X. R. Cao, W. Zhou and H. G. Fu, *CrystEngComm*, 2013, **15**, 5144-5149.
- 26 L. Zhao, F. Q. Tao, Z. Quan, X. L. Zhou, Y. H. Yuan and J. C. Hu, *Mater. Lett.*, 2012, **68**, 28-31.
- 27 X. Y. Chen, Z. H. Wang, X. Wang, R. Zhang, X. Y. Liu, W. J. Lin and Y. T. Qian, *J. Cryst. Growth*, 2004, **263**, 570-574.
- 28 J. Liu and D. F. Xue, *J. Cryst. Growth*, 2009, **311**, 500-503.
- 29 A. Y. Satoh, J. E. Trosko and S. J. Masten, *Environ. Sci. Technol.*, 2007, **41**, 2881-2887.
- 30 Z. Li, L. W. Mi, W. H. Chen, H. W. Hou, C. T. Liu, H. L. Wang, Z. Zheng and C. Y. Shen, *CrystEngComm*, 2012, **14**, 3965-3971.
- 31 W. W. He, H. M. Jia, X. X. Li, Y. Lei, J. Li, H. X. Zhao, L. W. Mi, L. Z. Zhang and Z. Zheng, *Nanoscale*, 2012, **4**, 3501-3506.
- 32 L. W. Mi, W. T. Wei, Z. Zheng, G. S. Zhu, H. W. Hou, W. H. Chen and X. X. Guan, *Nanoscale*, 2013, DOI: 10.1039/c3nr04923j.
- 33 L. W. Mi, Z. Li, W. H. Chen, Q. Ding, Y. F. Chen, Y. D. Zhang, S. S. Guo, H. M. Jia, W. W. He and Z. Zheng, *Thin Solid Films*, 2013, **534**, 22-27.
- 34 L. S. Zhong, J. S. Hu, H. P. Liang, A. M. Cao, W. G. Song and L. J. Wan, *Adv. Mater.*, 2006, **18**, 2426-2431.
- 35 J. S. Hu, L. S. Zhong, W. G. Song and L. J. Wan, *Adv. Mater.*, 2008, **20**, 2977-2982.
- 36 M. Basu, A. K. Sinha, M. Pradhan, S. Sarkar, Y. Negishi, G. and T. Pal, *Environ. Sci. Technol.*, 2010, **44**, 6313-6318.
- 37 F. Li, J. F. Wu, Q. H. Qin, Z. Li and X. T. Huang, *Powder Technol.*, 2010, **198**, 267-274.
- 38 S. He, G. S. Wang, C. Lu, X. Luo, B. Wen, L. Guo and M. S. Cao, *ChemPlusChem*, 2013, **78**, 250-258.
- 39 J. R. Huang, Y. Y. Wang, C. P. Gu and M. H. Zhai, *Mater. Lett.*, 2013, **99**, 31-34.
- 40 M. R. Wang, F. Xie, W. J. Li, M. F. Chen and Y. Zhao, *J. Mater. Chem. A*, 2013, **1**, 8616-8621.
- 41 X. Y. Meng, G. H. Tian, Y. J. Chen, R. T. Zhai, J. Zhou, Y. H. Shi, X. R. Cao, W. Zhou and H. G. Fu, *CrystEngComm*, 2013, **15**, 5144-5149.
- 42 C. H. Deng, H. M. Hu, X. Q. Ge, C. L. Han, D. F. Zhao and G. Q. Shao, *Ultrason. Sonochem.*, 2011, **18**, 932-937.
- 43 K. V. Singh, A. A. Martinez-Morales, G. T. S. Andavan, K. N. Bozhilov and M. Ozkan, *Chem. Mater.*, 2007, **19**, 2446-2454.
- 44 S. Komarneni, Q. H. Li and R. Roy, *J. Mater. Chem.*, 1994, **4**, 1903-1906.
- 45 S. M. Ou, Q. Xie, D. K. Ma, J. B. Liang, X. K. Hu, W. C. Yu and Y. T. Qian, *Mater. Chem. Phys.*, 2005, **94**, 460-466.
- 46 K. S. W. Sing, D. H. Everett, R. A. W. Haul, L. Moscou, R. A. Pierotti, J. Rouquerol and T. Siemieniewska, *Pure Appl. Chem.*, 1985, **57**, 603-619.
- 47 L. W. Mi, W. T. Wei, Z. Zheng, Y. Gao, Y. Liu, W. H. Chen and X. X. Guan, *Nanoscale*, 2013, **5**, 6589-6598.
- 48 C. H. Deng and X. B. Tian, *Mater. Res. Bull.*, 2013, **48**, 4344-4350.
- 49 R. Vijaya Kumar, Y. Diamant and A. Gedanken, *Chem. Mater.*, 2000, **12**, 2301-2305.
- 50 M. Kristl, N. Hojnik, S. Gyergyek and M. Drogenik, *Mater. Res. Bull.*, 2013, **48**, 1184-1188.



Graphic Abstract:



Hollow CuS architectures have been fabricated via a template-free and green sonochemical process displaying superior Fenton-like catalytic activities.